1   ***In situ* activation and heterologous production of a cryptic lantibiotic from a**
2   **plant-ant derived *Saccharopolyspora* species**

3

4   Eleni Vikeli,[1,2#] David A. Widdick,[1#] Sibyl F. Batey,[1#] Daniel Heine,[1] Neil A. Holmes,[2]
5   Mervyn J. Bibb,[1] Dino J. Martins,[3,4] Naomi E. Pierce,[3] Matthew I. Hutchings[2]* and
6   Barrie Wilkinson[1]*

7

8   [1]Department of Molecular Microbiology, John Innes Centre, Norwich Research Park,
9   Norwich NR4 7UH, UK

10   [2]School of Biological Sciences, University of East Anglia, Norwich NR4 7TJ, UK

11   [3]Department of Organismic and Evolutionary Biology, Harvard University, Cambridge
12   MA 02138, USA

13   [4]Mpala Research Centre, P O Box 555, Nanyuki, 10400 Kenya

14

15   *Address correspondence to Barrie Wilkinson (barrie.wilkinson@jic.ac.uk) and
16   Matthew I. Hutchings (m.hutchings@uea.ac.uk). [#]These authors contributed equally
17   to this work

18

19   **Abstract.** Most clinical antibiotics are derived from actinomycete natural products
20   (NPs) discovered at least 60 years ago. Repeated rediscovery of known compounds
21   led the pharmaceutical industry to largely discard microbial NPs as a source of new
22   chemical diversity but advances in genome sequencing revealed that these organisms
23   have the potential to make many more NPs than previously thought. Approaches to
24   unlock NP biosynthesis by genetic manipulation of the strain, by the application of
25   chemical genetics, or by microbial co-cultivation have resulted in the identification of
26   new antibacterial compounds. Concomitantly, intensive exploration of coevolved
27   ecological niches, such as insect-microbe defensive symbioses, has revealed these
28   to be a rich source of chemical novelty. Here we report the novel lanthipeptide
29   antibiotic kyamicin generated through the activation of a cryptic biosynthetic gene

30 cluster identified by genome mining *Saccharopolyspora* species found in the obligate

31 domatia-dwelling ant *Tetraponera penzigi* of the ant plant *Vachellia drepanolobium*.

32 Heterologous production and purification of kyamicin allowed its structural

33 characterisation and bioactivity determination. Our activation strategy was also

34 successful for the expression of lantibiotics from other genera, paving the way for a

35 synthetic heterologous expression platform for the discovery of lanthipeptides that are

36 not detected under laboratory conditions or that are new to nature.

37

38 **Importance.** The discovery of novel antibiotics to tackle the growing threat of

39 antimicrobial resistance is impeded by difficulties in accessing the full biosynthetic

40 potential of microorganisms. The development of new tools to unlock the biosynthesis

41 of cryptic bacterial natural products will greatly increase the repertoire of natural

42 product scaffolds. Here we report an activation strategy that can be rapidly applied to

43 activate the biosynthesis of cryptic lanthipeptide biosynthetic gene clusters. This

44 allowed the discovery of a new lanthipeptide antibiotic directly from the native host and

45 via heterologous expression.

46

47   Antimicrobial resistance (AMR) is arguably the greatest health threat facing humanity
48   in the 21st century (1-3). It is predicted that without urgent action, infectious disease
49   will become the biggest killer of humans by 2050 (1). The majority of clinically used
50   antibiotics are based on microbial natural products, isolated mostly from soil-dwelling
51   *Streptomyces* species and other filamentous actinomycete bacteria, and these
52   organisms remain a promising source of new antibiotics. Although the discovery
53   pipeline began to dry up in the 1960s, blighted by the rediscovery of known
54   compounds, we know from large scale genome sequencing that up to 90% of microbial
55   natural products are not produced under laboratory conditions (4). Thus, there exists
56   a wealth of novel chemistry waiting to be discovered by mining the genomes of these
57   organisms. Bearing in mind that >600 *Streptomyces* species and many other so called
58   'rare' actinomycetes have been described, thousands of potentially useful but "cryptic"
59   bioactive compounds are waiting to be discovered, even from well-characterised
60   strains (5,6). Several approaches have been taken to activate cryptic pathways
61   including the heterologous expression of entire biosynthetic gene clusters (BGCs) in
62   optimised *Streptomyces* host strains, and rewiring BGCs to bypass their natural
63   regulatory mechanisms (7). The knowledge that we have barely sampled the
64   biosynthetic capabilities of known strains, and that even well explored environments
65   such as soil have been under sampled for antibiotic-producing microbes, provides a
66   much-needed opportunity for the development of new natural product-based
67   antibiotics.

68   Searching symbiotic niches for new actinomycete strains also shows great promise
69   for discovering new natural products (8-11). We previously described the
70   formicamycins, new polyketides with potent Gram-positive antibacterial activity
71   produced by a new *Streptomyces* species that we named *Streptomyces formicae* KY5
72   (12). This species was isolated from a phytoecioius ant species, *Tetraponera penzigi*,
73   whose colonies inhabit the African ant plant *Vachellia (=Acacia) drepanolobium*. The
74   ants were collected in Kenya, hence the KY strain designation (13). These ants live in
75   symbiosis with their host plants, the "whistling thorn acacias", that have evolved
76   specialised hollow, stipular thorns called domatia to house the ants (14). In return for
77   housing, plant ants protect their hosts against attack by large herbivores, including
78   elephants (15), and recent reports have suggested that they grow specialized fungal
79   communities inside their domatia, possibly as a food source for their larvae (16,17).

80   The external, cuticular microbiome of *T. penzigi* ants is heterogeneous, and unbiased

81   methods have shown this is dominated by members of the phyla Proteobacteria and

82   Firmicutes, with Actinobacteria forming a minor component (13). This contrasts with

83   the better studied fungus-farming leafcutter ants of the tribe Attini, which are

84   dominated by actinobacteria, specifically by a single strain of *Pseudonocardia* that can

85   be vertically transmitted by the new queens (18,19). Leafcutter ants feed cut plant

86   material to their symbiotic food fungus *Leucoagaricus gongylophorus* and use

87   antifungals made by their *Pseudonocardia* symbionts to defend their food fungus

88   against fungal parasites in the genus *Escovopsis* (20-22). Despite the low abundance

89   of actinobacteria, we isolated several strains, including three from the rare

90   actinomycete genus *Saccharopolyspora*, which, despite the modest number of

91   described species, is the origin of the medically and agriculturally important natural

92   products erythromycin and spinosyn.

93   Genome mining of these *Saccharopolyspora* strains identified a conserved BGC

94   encoding a putative cinnamycin-like lanthipeptide antibiotic (lantibiotic) (23), although

95   no products for this BGC could be identified from the wild-type isolates. Cinnamycin is

96   a class II type B lantibiotic produced by *Streptomyces cinnamoneus* DSM 40005 which

97   destabilises the cytoplasmic membrane by binding phosphatidylethanolamine (PE)

98   (23-25). Lanthipeptides belong to the ribosomally synthesised and post-translationally

99   modified peptide (RiPP) family of natural products (26,27), and cinnamycin is the

100   founding member of a sub-group of lanthipeptide RiPPs with antibacterial activity that

101   includes cinnamycin B (28), duramycin (29), duramycin B and C (30), and

102   mathermycin (31) (Fig. 1A). These molecules are produced by actinomycetes and

103   comprise 19 amino acid residues, several of which are modified to generate

104   lanthionione or methyllanthionine cross-links (26,27). Additional modifications include

105   β-hydroxylation of the invariant aspartic acid residue at position 15 and formation of

106   an unusual lysinoalanine cross-link between the serine residue at position 6 and lysine

107   residue at position 19 (32-34). The interaction of these molecules with PE has

108   therapeutic potential: duramycin binds to human lung epithelial cell membranes

109   leading to changes in the membrane, or its components, promoting chloride ion

110   secretion and clearance of mucus from the lungs (25). On this basis, duramycin

111   entered Phase II clinical trials for the treatment of cystic fibrosis (35).

4

112 Here we describe activation of the cryptic *Saccharopolyspora* lanthipeptide BGCs and

113 the characterization of their product, a new class II lantibiotic that we called kyamicin.

114 We also exemplify a heterologous expression platform for lanthipeptide production that

115 may be particularly useful for strains that are refractory to genetic manipulation. The

116 methodologies reported should be applicable for the activation of cryptic BGCs from a

117 wide range of actinomycetes.

118

119 **RESULTS**

120 **Origin, characteristics and genome sequencing of *Saccharopolyspora* strains.**

121 The *Saccharopolyspora* strains were isolated from ants taken from the domatia of *T.*

122 *penzigi* plant ants collected in two locations in Kenya (13), and named KY3, KY7 and

123 KY21. 16S rDNA was amplified and Sanger sequenced using the universal primers

124 533F and 1492R (Genbank accession numbers JX306001, JX306003, JX306004,

125 respectively). Alignments show that KY3 and KY7 are identical across the sequenced

126 16S rDNA region while KY21 differs by a single base pair (Fig. S1). Further analysis

127 showed that all three strains share 99% sequence identity with *Saccharopolyspora*

128 16S rDNA sequences in public databases. High molecular weight genomic DNA was

129 isolated from each strain, sequenced at the Earlham Institute (Norwich, UK) using

130 SMRT sequencing technology (Pacific Biosciences RSII platform) and assembled

131 using the HGAP2 pipeline as described previously (36). This gave three circular

132 chromosomes of approx. 6.33 Mbp, the full analysis of which will be reported

133 separately. Alignment of the KY3 and KY7 genome sequences using RAST SEED

134 Viewer and BLAST dot plot revealed a full synteny along their genomes with 99-100%

135 sequence identity at the nucleotide level suggesting KY3 and KY7 are the same strain

136 and different to KY21.

137

138 **Identification of a conserved cinnamycin-like BGC.** The biosynthetic potential of

139 all three strains was probed using the genome mining platform antiSMASH (37). The

140 three genomes each encode approximately 25 BGCs with significant overlap.

141 Amongst these was a BGC for a cinnamycin-like lanthipeptide. The BGC architecture

142 was conserved across all three genomes, including an identical pro-peptide sequence

143 encoded by the precursor peptide gene, suggesting they all encode the same

144   molecule which we named kyamicin (Fig. 1B). The sequence and annotations for
145   these three BGCs have been deposited at GenBank under the accession numbers
146   MK251551 (KY3), MK251552 (KY7) and MK251553 (KY21).

147   Through comparison to the cinnamycin BGC (24), and cinnamycin biosynthesis (32),
148   we assigned roles to each of the genes in the kyamicin (*kya*) BGC (Table 1). The *kya*
149   BGC is more compact than that for cinnamycin, and the genes missing from the
150   kyamicin BGC are dispensable for cinnamycin production (38). The *cinorf11* gene is
151   not required for cinnamycin production but a homologue is present in the kyamicin
152   cluster. While *cinorf11* lacks a plausible stop codon and its reading frame extends 570
153   bp into the *cinR1* gene, its homologue, *kyaorf11*, has a stop codon and does not run
154   into the *kyaR1* gene suggesting it may encode a functional protein.

155   To detect production of kyamicin we grew all three strains on a range of 13 liquid media
156   (Table S2) and extracted after four, five, six and seven days of growth, using
157   (individually) methanol and ethyl acetate. Analysis of the extracts using UPLC/MS
158   failed to identify the anticipated product (the methods were validated using authentic
159   duramycin). This was consistent with parallel bioassays which failed to show any
160   antibacterial activity for the extracts against *Bacillus subtilis* EC1524, which is sensitive
161   to cinnamycin (24). Similarly, no activity was observed in overlay bioassays.

162   **Activation of the kyamicin BGC.** Cinnamycin production and self-immunity
163   ultimately rely on two gene products (38). The transcription of the biosynthetic genes
164   is driven by CinR1, a SARP (*Streptomyces* Antibiotic Regulatory Protein, which usually
165   act as pathway specific transcription activators), and self-immunity is conferred by a
166   methyl transferase (Cinorf10) that modifies PE in the membrane to prevent binding of
167   cinnamycin. We reasoned that transcription of the homologues of these two genes
168   (*kyaR1* and *kyaL*, respectively), driven by a constitutive promoter, would circumvent
169   the natural regulatory mechanism and initiate production of kyamicin. To achieve this,
170   we made a synthetic construct, pEVK1, containing *kyaR1-kyaL* (in that order), with a
171   *Nde*I site overlapping the start codon of *kyaR1*, a *Hin*dIII site after the stop codon of
172   the *kyaL* and with the *kyaN* ribosome binding site (RBS) located between the two
173   genes (the *kyaN* RBS was chosen as its sequence is most similar in the BGC to that
174   of an ideal RBS) (Fig. S2A). The *kyaR1-kyaL* cassette was cloned into pGP9 (39) to
175   yield pEVK4 which was introduced into the three *Saccharopolyspora* strains by

6

176   conjugation. This resulted in single copies of the plasmid integrated at the φBT1 phage

177   integration site of each strain. Exconjugants were assayed by overlaying with *B.*

178   *subtilis* EC1524, revealing zones of clearing for all three strains containing pEVK4 (Fig.

179   2A, Fig. S3). For the KY21 ex-conjugant, agar plugs were taken from the zone of

180   clearing, extracted with 5% formic acid and analysed by UPLC/MS (Fig. 2A). In

181   contrast to the relevant controls, an ion at *m/z* 899.36 was observed corresponding to

182   the expected $[M + 2H]^{2+}$ ion of kyamicin (Table 2).

183   **Heterologous expression of the kyamicin BGC.** Attempts to scale up cultures of

184   *Saccharopolyspora* sp. KY21/pEVK4 to generate sufficient material for further study

185   were not successful. Consequently, we attempted heterologous expression of the *kya*

186   BGC in the well-established host *Streptomyces coelicolor* M1152 (40). To achieve this,

187   we cloned *kyaR1L* as a *Nde*I/*Hin*dIII fragment into pIJ10257, a φBT1-based integrative

188   expression vector with a hygromycin resistance marker (41); this yielded pEVK6,

189   which has the constitutive *ermE** promoter driving expression of *kyaR1L*. We then

190   commissioned a synthetic operon containing *kyaN-H* plus the upstream promoter

191   region of *kyaN* as an *Eco*RI/*Xba*I fragment (Fig. S2B). This was cloned into pSET152

192   (42) to give pWDW63, which integrates into the *S. coelicolor* chromosome at the φC31

193   integration site, conferring apramycin resistance. pEVK6 and pWDW63 were then

194   introduced sequentially into *S. coelicolor* M1152 *via* conjugation, and apramycin plus

195   hygromycin resistant ex-conjugants were grown on R5 agar and overlaid with *B.*

196   *subtilis* EC1524. In contrast to the control strains, these gave a pronounced zone of

197   clearing. Agar plugs were taken from the zone of clearing, extracted and analysed by

198   UPLC/MS, revealing the expected $[M + 2H]^{2+}$ ion for kyamicin which was not present

199   in the controls (Fig. 2B). In addition to kyamicin, a second minor new compound was

200   observed with an *m/z* value of 891.36, consistent with the production of a small amount

201   of deoxykyamicin presumably reflecting incomplete β-hydroxylation of the aspartic

202   acid residue at position 15 (Table 2 and Fig. S4).

203   Having established the production of kyamicin in the M1152 heterologous host, we

204   used this system to better understand how each gene product contributes to the

205   activation of kyamicin biosynthesis. We cloned *kyaL* and *kyaR1* separately into

206   pIJ10257, to give pEVK12 and pEVK13, respectively. Each plasmid was then

207   introduced into M1152 alongside pWDW63, and doubly antibiotic resistant ex-

208   conjugants were selected. These were grown on R5 agar plates and overlaid with *B.*

7

209   *subtilis* EC1524; agar plugs were extracted from the resulting bioassay plates as

210   before. For M1152/pEVK12 (*kyaL* only) no growth inhibition of the bioassay strain was

211   observed and we could not detect kyamicin or deoxykyamicin using UPLC/MS. For

212   M1152/pEVK13 (*kyaR1* only), we observed a zone of inhibition which was

213   approximately three times smaller than for the M1152/pEVK6 (*kyaR1L*) positive

214   control. UPLC/MS analysis of the M1152/pEVK13 strain detected only deoxykyamicin

215   (Fig. S4). This is consistent with previous work which reported that deoxy versions of

216   lantibiotics have lower biological activity (43).

217   **Isolation, structure elucidation and bioactivity.** To isolate and verify the structure

218   of kyamicin, growth of *S. coelicolor* M1152/pEVK6/pWDW63 was scaled up in liquid

219   culture and the cell pellet extracted with 50% methanol. Crude extracts were further

220   purified using semi-preparative HPLC to yield pure kyamicin (2.5 mg).

221   As the methyllanthionine bridges of kyamicin limit the ability to induce fragmentation

222   in MS/MS experiments, the lantibiotic was subjected to chemical reduction with

223    $NaBH_4$-$NiCl_2$ using a procedure published previously for the related molecule

224   cinnamycin B (28). This leads to removal of the methyllanthionine bridges and, as

225   anticipated, UPLC/MS of the product molecule showed an $[M + 2H]^{2+}$ ion at *m/z* 854.42

226   corresponding to the loss of three sulfur atoms and gain of six hydrogen atoms (Table

227   2 and Fig. 3). Tandem MS experiments were carried out using both ESI and MALDI-

228   ToF methods. Whilst ESI gave a complex mixture of fragmentation ions, for MALDI-

229   ToF the *y* ion (NH_3^+) series could be clearly observed, with fragmentation at the

230   lysinoalanine bridge appearing to occur via a rearrangement to give a glycine residue

231   at position 6 and $N=CH_2$ at the end of the lysine side chain (Fig. S5). The connectivity

232   of the peptide was consistent with the primary sequence of kyamicin predicted by our

233   bioinformatics analysis.

234   The chemical structure was further examined by NMR experiments comprising ^1H,

235   HSQC, TOCSY and NOESY analyses. Overall, 14 spin systems could be partially or

236   completely identified in the TOCSY spectrum. These could be putatively assigned

237   based on their spatial relationship determined from the NOESY spectrum. Coupling in

238   the HSQC spectrum then allowed identification of several C atoms in the molecule.

239   Spectra and assignments can be found in Fig. S6 and Table S3.

240   The bioactivity of the purified compound was compared with cinnamycin and

241   duramycin using the spot-on-lawn method. The minimum inhibitory concentration

242   (MIC) of kyamicin against *B. subtilis* EC1524 was 128 µg/mL, whereas duramycin

243   inhibited at 32 µg/mL and cinnamycin at 16 µg/mL, representing a 4 and 8-fold MIC

244   increase respectively (Fig. 4).

245   **Cross species activation of the duramycin BGC**. Many cinnamycin-like BGCs can

246   be identified in the published sequence databases, but their products remain cryptic.

247   Thus, the potential of the *kyaR1-kyaL* construct to induce expression of other

248   cinnamycin-like lantibiotics was explored.

249   The BGC for duramycin was cloned previously from *Streptomyces cinnamoneus*

250   ATCC 12686 (Fig. S7A) but attempts to produce the lantibiotic heterologously failed.

251   Consequently, the duramycin BGC was reconfigured in pOJKKH, which contains all

252   the biosynthetic genes, but lacks immunity and regulatory genes, and has a SARP

253   binding site upstream of *durN* that is similar to that upstream of *kyaN* (Fig. S7B) (38).

254   pOJKKH and pEVK6 were introduced sequentially into *S. coelicolor* M1152 *via*

255   conjugation and the resulting ex-conjugants assessed for duramycin production.

256   Overlay bioassays using *B. subtilis* EC1524 indicated the production of an antibacterial

257   molecule by *S. coelicolor* M1152/pOJKKH/pEVK6 (Fig. 5). Agar within the growth

258   inhibition zone was extracted and the resulting sample analysed by UPLC/MS. An ion

259   at *m/z* 1006.92 was observed, corresponding to the expected $[M + 2H]^{2+}$ ion for

260   duramycin (Table 2). The production of duramycin was confirmed by comparison to

261   an authentic standard. A deoxy derivative was also detected with an *m/z* of 998.93

262   (Table 2), typically at ~30% the level of duramycin. Expression of pOJKKH alone or in

263   conjunction with the empty pIJ10257 vector did not result in duramycin biosynthesis,

264   demonstrating that expression of both *kyaR1* and *kyaL* are required to induce

265   heterologous duramycin biosynthesis in *S. coelicolor* M1152. Thus, we have shown

266   that the SARP and resistance genes from a cinnamycin-like BGC from a

267   *Saccharopolyspora* species can be used to activate a cinnamycin-like BGC from a

268   *Streptomyces* species, a cross genus activation.

269

270

271

DISCUSSION

Three isolates from the relatively rare actinomycete genus *Saccharopolyspora* were isolated from the external microbiome of *T. penzigi* plant ants collected at two locations in Kenya more than 50 km apart (13). Despite this geographical separation, their genomes were extremely similar and analysis using antiSMASH identified almost identical biosynthetic capabilities. Amongst the conserved BGCs was one encoding a cinnamycin-like lantibiotic which we named kyamicin.

Despite culturing on a wide range of media, we were unable to elicit production of kyamicin in the wild-type *Saccharopolyspora* strains. The production of cinnamycin in *S. cinnamoneus* DSM 40005 requires the expression of two key genes, *cinR1* and *cinorf10*, encoding a pathway specific regulatory gene (a SARP) and a self-immunity gene (a PE methyltransferase), respectively (38). As the *kya* BGC encodes homologues of these genes, we expressed them constitutively in the three *Saccharopolyspora* strains which led to activation of the BGC and production of kyamicin. Since we were unable to isolate enough kyamicin from these strains for further study, a heterologous production platform was developed using *S. coelicolor* M1152 which allowed us to confirm the structure of kyamicin and assess its antibacterial activity.

Having demonstrated the utility of a constitutively expressed SARP/self-immunity cassette for driving expression of the otherwise silent *kya* BGC we utilised this knowledge to activate duramycin production in a heterologous host. Contemporaneous with our experiments, the duramycin BGC was also identified by genome sequencing of *S. cinnamoneus* ATCC 12686 (33). This analysis described the same genomic region containing *durN* to *durH* and surrounding genes (Table 1) but failed to reveal putative regulatory and immunity genes. Co-expression of *durA*, *durM*, *durN* and *durX* in *E. coli* was sufficient to direct the biosynthesis of duramycin A, and the functions of DurA, DurM, DurN and DurX were confirmed by detailed biochemical analyses. Our subsequent bioinformatic analysis of the published genome sequence identified homologs of the resistance genes *cinorf10*/*kyaL* and the regulatory genes *cinRKR1*/*kyaRKR1* in region 54637 to 59121 bp of contig MOEP01000113.1 from the deposited genome sequence (accession no. NZ_MOEP00000000). This region is separated from the *dur* biosynthetic genes by a

10

304 section of low mol %GC DNA, the analysis of which suggests that a phage or other
305 mobile element may have inserted between *durZ* and *durorf8* (Fig. S7). Thus, it
306 appears likely that the immunity and regulatory mechanisms described previously for
307 the control of cinnamycin biosynthesis are conserved for duramycin biosynthesis in *S.*
308 *cinnamoneus* ATCC 12686.

309 Given the potential utility of cinnamycin-like class II lanthipeptides in several
310 therapeutic contexts, the ability to generate analogues of these compounds with
311 modified properties and in sufficient quantity for preclinical assessment is of significant
312 value. The methods described here provide a platform for the identification of
313 additional natural lanthipeptides whose biosynthesis cannot be detected in the host
314 strain, and for the diversification of their chemical structures to generate new-to-nature
315 molecules.

316

317 MATERIALS AND METHODS

318 **Bacterial strains, plasmids and growth conditions.** All bacterial strains and
319 plasmids used in this study are listed in Table S1 in the supplemental material.
320 *Saccharopolyspora* and *Streptomyces* strains were grown on soya flour mannitol
321 (SFM) agar medium with appropriate antibiotics at 30 °C unless otherwise stated. *E.*
322 *coli* and *B. subtilis* EC1524 strains were grown on lysogeny broth (LB) medium with
323 appropriate antibiotics at 37 °C. R5 agar (44) was used for bioassay plates.

324 **DNA extraction and genomic analysis.** The salting out method (44) was used to
325 extract genomic DNA. The DNA was sequenced at the Earlham Institute (Norwich,
326 UK) using SMRT sequencing technology (Pacific Biosciences RSII platform) and
327 assembled using the HGAP2 pipeline (36).

328 **Overlay bioassays.** For each strain to be tested, a streak from a spore stock was
329 applied in the centre of an R5 agar plate and left to grow for seven days. *B. subtilis*
330 EC1524 was grown from a single colony overnight, then diluted 1:20 in fresh media
331 and grown until OD_{600} = 0.4 - 0.6. The exponential culture was mixed with 1:100 molten
332 soft nutrient agar (SNA) (44) and the mixture was used to overlay the plate (5 mL SNA
333 mixture/agar plate). The plate was incubated at room temperature overnight.

11

334 **Extractions from overlay bioassays.** Plugs of agar 6.35 mm in diameter were taken

335 adjacent to the streaked actinomycete strain on an overlay bioassay plate,

336 corresponding to the zone of growth inhibition where one was observed. Agar plugs

337 were frozen at -80 °C for 10 min, thawed and then 300 µL of 5% formic acid was

338 added. This was vortexed briefly and shaken for 20 min. After centrifugation (15,682

339 × g for 15 min) the supernatant was collected and filtered using a filter vial (HSTL

340 Labs) prior to UPLC-MS analysis.

341 **UPLC-HRMS.** Data were acquired with an Acquity UPLC system (Waters) equipped

342 with an Acquity UPLC® BEH C18 column, 1.7 µm, 1x100 mm (Waters) connected to

343 a Synapt G2-Si high-resolution mass spectrometer (Waters). For analytical UPLC 5.0

344 µL of each sample was injected and eluted with mobile phases A (water/0.1% formic

345 acid) and B (acetonitrile/0.1% formic acid) at a flow rate of 80 µL/min. Initial conditions

346 were 1% B for 1.0 min, ramped to 40 % B within 9.0 min, ramped to 99 % B within

347 1.0 min, held for 2 min, returned to 1 % B within 0.1 min and held for 4.9 min.

348 MS spectra were acquired with a scan time of 1.0 s in the range of $m/z = 50 - 2000$ in

349 positive resolution mode. The following parameters were used: capillary voltage of 3.0

350 kV, cone voltage 40 V, source offset 80 V, source temperature 130 °C, desolvation

351 temperature 350 °C, desolvation gas flow of 700 L/h. A solution of sodium formate was

352 used for calibration. Leucine encephalin peptide (H_2O/MeOH/formic acid:

353 49.95/49.95/0.1) was used as lock mass (556.2766 m/z) and was injected every 30 s

354 during each run. The lock mass correction was applied during data analysis.

355 **Design of *kya* BGC activation and immunity plasmids.** pEVK1, a pUC57 derivative,

356 contains the synthetic *kyaR1* and *kyaL* (Genscript) arranged as an operon. pEKV1 has

357 a *Nde*I site overlapping the start codon of *kyaR1* and a *Hin*dIII site immediately after

358 the stop codon of *kyaL* with the two genes separated by a short intergenic region

359 containing a RBS designed from the RBS of *cinN* (Fig. S2A). The *Nde*I-*Hin*dIII *kyaR1L*

360 fragment from pEVK1 was cloned in pGP9 (39) to give pEVK4, and into pIJ10257 (41)

361 to give pEKV6. *kyaR1* and *kyaL* were amplified individually as *Nde*I-*Hin*dIII compatible

362 fragments using the primers AmplkyaR1-F

363 (GCGCAAGCTTCTACGACGCGGTGTGA) and AmplkyaR1-R

364 (GCGCGCCATATGAAACCGCTGTCGTTCC) for *kyaR1*, and AmplkyaL-F

365 (GCGCGCCATATGGATCCAGTACAGACCA) and AmplkyaL-R

366 (GCGCAAGCTTTCAGCGGTCCTCCGCC) for *kyaL*; they were cloned as *Nde*I-*Hin*dIII

367 fragments into pIJ10257 to yield pEVK12 and pEVK13 respectively. PCR generated

368 fragments were verified by Sanger sequencing.

369 **Cloning the duramycin BGC from *Streptomyces cinnamoneus* ATCC 12686.** The

370 cloning of a ~5 Kb *Bgl*II fragment of chromosomal DNA to create pIJ10100 was

371 described previously (24). This plasmid has a *Kpn*I site in the middle of *durX*. *Kpn*I

372 fragments upstream and downstream of this *Kpn*I site were identified by Southern

373 blotting and isolated by creating a mini-library of *Kpn*I fragments in pBluescriptIIKS

374 followed by colony hybridization to give pDWCC2 and pDWCC3, respectively.

375 Analysis of the sequence of these plasmids identified 15 genes (shown in Fig. S7). A

376 plasmid carrying the duramycin biosynthetic genes but not the putative phage DNA

377 was prepared by digesting pDWCC3 with *Xho*I and *Hin*dIII (site is in the multiple

378 cloning site of pBluescriptIIKS) removing the 5' end of *durZ* and the putative phage

379 DNA. This region was replaced with a *Xho*I and *Hin*dIII cut PCR fragment that

380 reconstituted the portion of *durZ* removed in the previous step and introduced a *Hin*dIII

381 site upstream of the *durZ* start codon. The 666 bp PCR fragment was generated using

382 the primers BK10 (GAGCTTGACGCCGCCGAAGTAGC) and Hindprim

383 (GCGGCGAAGCTTGAGGTGGCCTCCTCCACGAAGCCA) with pDWCC3 as

384 template and was cut with *Xho*I plus *Hin*dIII to give a 363 bp fragment. The resulting

385 plasmid was then digested with *Kpn*I plus *Xba*I (the *Xba*I site is in the multiple cloning

386 site of pBluescriptIIKS) and the fragment carrying putative duramycin genes was

387 cloned into *Kpn*I plus *Xba*I cleaved pOJ436 to give pOJKH. The *Kpn*I fragment from

388 pDWCC2 was then cloned into pOJKH cut with *Kpn*I to give pOJKKH which was

389 verified by *Bgl*II digestion, thus restoring the original gene context.

390 **Isolation and purification of kyamicin.** *S. coelicolor* M1152/pWDW63/pEVK6 was

391 grown in tryptic soy broth (12 x 500 mL in 2.5 L Erlenmeyer flasks) and incubated at

392 28 °C and 200 rpm on an orbital shaker for seven days. The cells were harvested and

393 extracted with methanol/water (1:1; 500 mL) with ultrasonication for 2 h and

394 subsequent shaking for 16 h. After centrifugation, the supernatant was filtered and

395 concentrated under vacuum giving 613 mg of crude material, which was then purified

396 by semi-preparative HPLC. Chromatography was achieved over a Phenomenex

397 Gemini-NX reversed-phase column (C18, 110 Å, 150 × 21.2 mm) using a Thermo

398 Scientific Dionex UltiMate 3000 HPLC system. A gradient was used with mobile

13

399   phases of A: H_2O (0.1% formic acid) and B: methanol; 0–1 min 10% B, 1–35 min 10-

400   85% B, 35–40 min 85-100% B, 40–45 min 100% B, 45-45.1 min 100-10% B, 45.1-50

401   min 10% B; flowrate 20 mL/min; injection volume 1000 µL. Absorbance was monitored

402   at 215 nm and fractions (20 mL) were collected and analysed by UPLC/MS. Kyamicin

403   was observed in fractions 22-25 which were combined and concentrated to yield an

404   off-white solid (2.5 mg).

405   **Minimum inhibitory concentration (MIC) determination.** The spot-on-lawn method

406   was used to determine lantibiotic MICs. A 1000 µg/mL stock solution of each lantibiotic

407   was prepared using sterile water, along with serial dilutions from 256 – 8 µg/mL. *B.*

408   *subtilis* EC1524 was grown and mixed with molten SNA as described above to create

409   a lawn of bacterial growth. Once set, 5 µL of each dilution was applied directly to the

410   agar and incubated overnight at room temperature. The MIC was defined as the lowest

411   concentration for which a clear zone of inhibition was observed.

412   **Chemical reduction of kyamicin**. Kyamicin (1 mg) was dissolved in methanol (0.5

413   mL) and added to an aqueous solution of $NiCl_2$ (20 mg/mL; 0.5 mL). The solution was

414   mixed with solid $NaBH_4$ (5 mg), resulting in the generation of hydrogen gas and the

415   formation of a black Ni_2B precipitate. The tube was immediately sealed, and the

416   mixture stirred at 55 °C. The reaction progress was monitored by UPLC-HRMS as

417   described above, for which a peak with an *m/z* of 899.36 was observed for kyamicin

418   ($[M + 2H]^{2+}$). The successive formation of peaks with the following masses were

419   observed: *m/z* = 884.38, 869.40 and 854.42, corresponding to the successive

420   reduction of the three thioether bridges. After 5 h only the ion with *m/z* 854.42 could

421   be observed, indicating that the starting material had been completely reduced. The

422   precipitate was collected by centrifugation at 15,682 × *g* for 10 min. As the reaction

423   supernatant contained only trace amounts of the desired product, a fresh solution of

424   $MeOH/H_2O$ 1:1 (0.5 mL) was added to the precipitate and it was subject to

425   ultrasonication for 30 min. Reduced kyamicin was then detected in sufficient quantity

426   for MS/MS experiments to confirm the peptide sequence.

427   **MS analysis of reduced kyamicin**. For ESI/MS[2] analysis the mass of interest

428   (854.42) was selected using an inclusion list and fragmented using data directed

429   analysis (DDA) with the following parameters: top3 precursor selection (inclusion list

430   only); MS2 threshold: 50,000; scan time 0.5 s without dynamic exclusion. Collision

14

431 energy (CE) was ramped between 15-20 at low mass (50 *m/z*) and 40-100 at high
432 mass (2000 *m/z*). Further increase of the CE to 20-30/60-120 led to complete
433 fragmentation.

434 For MALDI-ToF/MS the samples were mixed with α-cyano-4-hydroxycinnamic acid as
435 matrix and analysed on an AutoflexTM Speed MALDI-TOF/TOF mass spectrometer
436 (Bruker DaltonicsTM GmbH). The instrument was controlled by a flexControlTM
437 (version 3.4, Bruker) method optimised for peptide detection and calibrated using
438 peptide standards (Bruker). For sequence analysis fragments produced by PSD were
439 measured using the LIFT method (Bruker). All spectra were processed in
440 flexAnalysisTM (version 3.4, Bruker).

441 **NMR experiments.** NMR measurements were performed on a Bruker Avance III
442 800 MHz spectrometer. Chemical shifts are reported in parts per million (ppm) relative
443 to the solvent residual peak of DMSO-d_6 (^{1}H: 2.50 ppm, quintet; ^{13}C: 39.52 ppm,
444 septet).

445

ACKNOWLEDGEMENTS

466

467   **FIGURE LEGENDS**

468   **FIG 1 Kyamicin peptide sequence and biosynthesis. (A)** Alignment of core

469   peptides of kyamicin and a selection of known Type B cinnamycin-like lantibiotics, with

470   the positions of the thioether and lysinoalanine bridges in the mature peptide shown.

471   Conserved residues are highlighted in green, similar residues are highlighted in grey.

472   **(B)** The kyamicin biosynthetic gene cluster, with genes colored according to predicted

473   function. **(C)** Schematic of kyamicin biosynthesis. The thioether bridges are formed

474   first by dehydration of Thr4, Thr11, Thr18 and Ser6 by KyaM to form dehydrobutyrine

475   (Dhb) and dehydroalanine (Dha) residues, respectively. After thioether cyclization by

476   KyaM, Dhb becomes S-linked Abu and Dha becomes S-linked Ala. Asp15 is

477   hydroxylated by KyaX and the lysinoalanine bridge is then formed between Dha6 and

478   Lys19 by KyaN. After the core peptide is fully modified, the leader peptide is

479   proteolytically cleaved. **(D)** Structural representation of the mature kyamicin lantibiotic.

480   **FIG 2 Activation of kyamicin biosynthesis and heterologous expression.** Overlay

481   bioassays were carried out with *B. subtilis* EC1524 and agar plugs were taken

482   adjacent to the central streak and analysed by UPLC/MS. Extracted ion

483   chromatograms are shown where *m/z* = 899.36 ([M + 2H]$^{2+}$). Images and LC traces

484   are representative of at least three biological repeats. **(A)** Activation of kyamicin

485   production in KY21 strains. The pEVK4 vector containing *kyaR1* and *kyaL* results in a

486   zone of inhibition, corresponding to the production of kyamicin, in contrast to the pGP9

487   empty vector control or the wildtype strain. **(B)** Heterologous expression of kyamicin

488   in *S. coelicolor* M1152. A zone of inhibition, corresponding to kyamicin production, is

489   observed only when the pWDW63 carrying the *kya* biosynthetic genes is expressed in

490   combination with pEVK6 carrying *kyaR1* and *kyaL.*

491   **FIG 3 Characterisation of kyamicin.** The connectivity of the peptide was confirmed

492   by chemical reduction followed by tandem MS fragmentation. Reduction with NaBH$_4$-

493   NiCl$_2$ resulted in the cleavage of the methyllanthionine bridges (blue), corresponding

494 to the loss of three S atoms and gain of six H atoms, with a mass shift from $[M + 2H]^{2+}$

495 = 899.36 *m/z* to 854.42 *m/z*. Tandem MS using the MALDI-ToF LIFT method allowed

496 identification of the *y* ion (NH_3^+) series for the complete peptide (Figure S5).

497 Fragmentation of the lysinoalanine bridge (pink) occurred via rearrangement to give

498 $N=CH_2$ at the terminus of the lysine sidechain and a glycine residue at position 6.

499 **FIG 4 Comparative bioassay of kyamicin, duramycin and cinnamycin against *B.***

500 ***subtilis* EC1524.** The MIC of each substance was determined by direct application of

501 serial dilutions of the compounds in water, on a SNA agar plate inoculated with *B.*

502 *subtilis* EC1524. NC = H_2O is the negative control. Kyamicin displays an MIC of 128

503 μg/mL, whereas duramycin inhibits at 32 μg/mL and cinnamycin at 16 μg/mL.

504 **FIG 5 Activation of duramycin biosynthesis.** Overlay bioassays were carried out

505 with *B. subtilis* EC1524 and agar plugs were taken adjacent to the central streak and

506 analysed by UPLC/MS. Extracted ion chromatograms are shown where *m/z* = 1006.93

507 ($[M+2H]^{2+}$). Duramycin was only detected in the strain carrying both pOJKHH and

508 pEVK6. The duramycin peak aligns with an authentic standard of duramycin (1 mg/mL

509 in 5% formic acid), shown on a separate scale. Images and LC traces are

510 representative of at least three biological repeats.

511

512 **TABLES**

513 **TABLE 1 Proteins encoded by the cinnamycin and kyamicin BGCs.**

514 **TABLE 2 Calculated and observed *m/z* values for lantibiotic compounds in this**

515 **study.**

516

517 **SUPPLEMENTAL MATERIAL**

518 **FIG S1 Alignment of *Saccharopolyspora* sp. KY3, KY7 and KY21 16S rDNA**

519 **sequences.** The alignment was performed with Clustal Omega (v1.2.4) and the figure

520 was generated by SnapGene Viewer (v4.2.11). The difference between KY21 to

521 strains KY3 and KY7 is indicated with a black arrow and a box at position 685.

17

522 **FIG S2 Schematic of synthetic artificial operons. (A)** The operon consisting of
523 *kyaR1*, encoding a *Streptomyces* antibiotic regulatory protein (SARP), and *kyaL*,
524 encoding a PE-methyl transferase that provides resistance – the homologues of *cinR1*
525 and *cinorf10* respectively. **(B)** The operon carrying genes *kyaN* to *kyaH* as an
526 *EcoRI/XbaI* fragment. These genes are expected to be essential for kyamicin
527 biosynthesis.

528 **FIG S3 Activation of kyamicin biosynthesis in KY3 and KY7.** The pEVK4 vector
529 containing *kyaR1* and *kyaL* results in a zone of inhibition, corresponding to the
530 production of kyamicin, in contrast to the pGP9 empty vector control or the wildtype
531 strain. **(A)** Activation of kyamicin production in KY3, and **(B)** in KY7.

532 **FIG S4 Dissection of the contribution of *kyaR1* and *kyaL* to kyamicin BGC**
533 **activation.** Overlay bioassays were carried out with *B. subtilis* EC1524 and agar plugs
534 were taken adjacent to the central streak and analysed by UPLC/MS. Expression of
535 *kyaL* (pEVK12) does not result in a zone of inhibition. Expression of *kyaR1* (pEVK1)
536 results in a zone of inhibition, corresponding to the production of deoxykyamicin only.
537 Co-expression of *kyaR1* and *kyaL* (pEVK6) results in a zone of inhibition,
538 corresponding to the production of both kyamicin and deoxykyamicin. Images and LC
539 traces are representative of at least three biological repeats. **(A)** Extracted ion
540 chromatograms are shown where *m/z* = 899.36 ($[M+2H]^{2+}$). **(B)** Extracted ion
541 chromatograms are shown where *m/z* = 891.36 ($[M+2H]^{2+}$).

542 **FIG S5 Kyamicin fragmentation.** Following reduction to remove methyllanthionine
543 bridges, kyamicin was subject to MALDI-ToF tandem MS, giving the complete *y* ion
544 (NH_3^+) series. **(A)** Structure of reduced kyamicin and the $y_1 - y_{18}$ ion series. **(B)** MALDI-
545 ToF tandem MS spectrum with the *y* ion series indicated with dashed red lines.

546 **FIG S6 Kyamicin NMR Spectra. (A)** ^{1}H NMR spectrum. **(B)** TOCSY spectrum. **(C)**
547 NOESY spectrum. **(D)** HSQC spectrum.

548 **FIG S7 Schematic of duramycin BGC and plasmids used to construct pOJKKH**
549 **and SARP binding sites of kyamicin, cinnamycin and duramycin. (A)** The *S.*
550 *cinnamoneus* DNA sequences represented on the plasmids pDWCC2 and pDWCC3
551 are present in the published genome sequence as 81593-99144 bp of contig
552 NZ_MOEP01000024.1. pDWCC2 consists of the area from the left side *Kpn*I site (from

553   *durorf1*) to the central side *Kpn*I site in *durX*. pDWCC3 consists of the area covering

554   from the central *Kpn*I site in *durX* to the right side *Kpn*I site after a putative integrase

555   encoding gene. The putative duramycin resistance/regulatory genes are represented

556   in the published genome sequence by 54637-59121 bp of contig

557   NZ_MOEP01000113.1. **(B)** Sequence alignment of putative SARP binding sites of

558   kyamicin, cinnamycin and duramycin. Conserved residues within all three sequences

559   are marked with asterisks and the 5 bp SARP binding motifs are in bold. The alignment

560   was performed with Clustal Omega (v1.2.4).

561

562   **TABLE S1 Strains and plasmids used in this work.**

563   **TABLE S2 Recipes for liquid screening media.** Quantities of components are given

564   in g/L. SM = screening media.

565   **TABLE S3 Putative NMR assignments**. ND = not determined.

566

567   **REFERENCES**

568   1.   O'Neill J, Davies S, Rex J, White L, Murray R. 2016. Review on antimicrobial

569   resistance, tackling drug-resistant infections globally: final report and

570   recommendations. London: Wellcome Trust and UK Government.

571   2.   Tacconelli E, Carrara E, Savoldi A, Harbarth S, Mendelson M, Monnet DL,

572   Pulcini C, Kahlmeter G, Kluytmans J, Carmeli Y, Ouellette M, Outterson K,

573   Patel J, Cavaleri M, Cox EM, Houchens CR, Grayson ML, Hansen P, Singh N,

574   Theuretzbacher U, Magrini N, Aboderin AO, Al-Abri SS, Awang Jalil N,

575   Benzonana N, Bhattacharya S, Brink AJ, Burkert FR, Cars O, Cornaglia G, Dyar

576   OJ, Friedrich AW, Gales AC, Gandra S, Giske CG, Goff DA, Goossens H,

577   Gottlieb T, Guzman Blanco M, Hryniewicz W, Kattula D, Jinks T, Kanj SS, Kerr

578   L, Kieny M-P, Kim YS, Kozlov RS, Labarca J, Laxminarayan R, Leder K, et al.

579   2018. Discovery, research, and development of new antibiotics: the WHO

580   priority list of antibiotic-resistant bacteria and tuberculosis. Lancet Infect Dis

581   18:318-327.

582   3.   Talkington K, Shore C, Kothari P. 2016. A scientific roadmap for antibiotic

583   discovery. The Pew Charitable Trust: Philadelphia, PA, USA.

584   4.   Doroghazi JR, Albright JC, Goering AW, Ju KS, Haines RR, Tchalukov KA,
585   Labeda DP, Kelleher NL, Metcalf WW. 2014. A roadmap for natural product
586   discovery based on large-scale genomics and metabolomics. Nat Chem Biol
587   10:963-8.

588   5.   Kämpfer P, Glaeser SP, Parkes L, van Keulen G, Dyson P. 2014. The Family
589   *Streptomycetaceae*. The Prokaryotes: Actinobacteria:889-1010.

590   6.   Nouioui I, Carro L, García-López M, Meier-Kolthoff JP, Woyke T, Kyrpides NC,
591   Pukall R, Klenk H-P, Goodfellow M, Göker M. 2018. Genome-Based
592   Taxonomic Classification of the Phylum *Actinobacteria*. Front Microbiol 9.

593   7.   Rutledge PJ, Challis GL. 2015. Discovery of microbial natural products by
594   activation of silent biosynthetic gene clusters. Nat Rev Microbiol 13:509.

595   8.   van der Meij A, Worsley SF, Hutchings MI, van Wezel GP. 2017. Chemical
596   ecology of antibiotic production by actinomycetes. FEMS Microbiol Rev 41:392-
597   416.

598   9.   Adnani N, Rajski SR, Bugni TS. 2017. Symbiosis-inspired approaches to
599   antibiotic discovery. Nat Prod Rep 34:784-814.

600   10.   Van Arnam EB, Currie CR, Clardy J. 2018. Defense contracts: molecular
601   protection in insect-microbe symbioses. Chem Soc Rev 47:1638-1651.

602   11.   Molloy EM, Hertweck C. 2017. Antimicrobial discovery inspired by ecological
603   interactions. Curr Opin Microbiol 39:121-127.

604   12.   Qin Z, Munnoch JT, Devine R, Holmes NA, Seipke RF, Wilkinson KA, Wilkinson
605   B, Hutchings MI. 2017. Formicamycins, antibacterial polyketides produced by
606   *Streptomyces formicae* isolated from African *Tetraponera* plant-ants. Chem Sci
607   8:3218-3227.

608   13.   Seipke RF, Barke J, Heavens D, Yu DW, Hutchings MI. 2013. Analysis of the
609   bacterial communities associated with two ant-plant symbioses.
610   Microbiologyopen 2:276-83.

611   14.   Young TP, Stubblefield CH, Isbell LA. 1996. Ants on swollen-thorn acacias:
612   species coexistence in a simple system. Oecologia 109:98-107.

613   15.   Riginos C, Karande MA, Rubenstein DI, Palmer TM. 2015. Disruption of a
614   protective ant-plant mutualism by an invasive ant increases elephant damage
615   to savanna trees. Ecology 96:654-61.

616   16.   Blatrix R, Djieto-Lordon C, Mondolot L, La Fisca P, Voglmayr H, McKey D.
617   2012. Plant-ants use symbiotic fungi as a food source: new insight into the
618   nutritional ecology of ant-plant interactions. Proc Biol Sci 279:3940-7.

619   17.   Baker CC, Martins DJ, Pelaez JN, Billen JP, Pringle A, Frederickson ME, Pierce
620   NE. 2017. Distinctive fungal communities in an obligate African ant-plant
621   mutualism. Proc Biol Sci 284.

622   18.   Currie CR. 2001. A Community of Ants, Fungi, and Bacteria: A Multilateral
623   Approach to Studying Symbiosis. Annu Rev Microbiol 55:357-380.

624   19.   Andersen SB, Hansen LH, Sapountzis P, Sørensen SJ, Boomsma JJ. 2013.
625   Specificity and stability of the *Acromyrmex–Pseudonocardia* symbiosis.
626   Molecular Ecology 22:4307-4321.

627   20.   Barke J, Seipke RF, Gruschow S, Heavens D, Drou N, Bibb MJ, Goss RJ, Yu
628   DW, Hutchings MI. 2010. A mixed community of actinomycetes produce
629   multiple antibiotics for the fungus farming ant *Acromyrmex octospinosus*. BMC
630   Biol 8:109.

631   21.   Cafaro MJ, Poulsen M, Little AE, Price SL, Gerardo NM, Wong B, Stuart AE,
632   Larget B, Abbot P, Currie CR. 2011. Specificity in the symbiotic association
633   between fungus-growing ants and protective *Pseudonocardia* bacteria. Proc
634   Biol Sci 278:1814-22.

635   22.   Heine D, Holmes NA, Worsley SF, Santos ACA, Innocent TM, Scherlach K,
636   Patrick EH, Douglas WY, Murrell JC, Vieria PC. 2018. Chemical warfare
637   between leafcutter ant symbionts and a co-evolved pathogen. Nat Commun
638   9:2208.

639   23.   Benedict RG, Dvonch W, Shotwell OL, Pridham TG, Lindenfelser LA. 1952.
640   Cinnamycin, an antibiotic from *Streptomyces cinnamoneus* nov. sp. Antibiot
641   Chemother 2:591-4.

642   24.   Widdick D, Dodd H, Barraille P, White J, Stein T, Chater K, Gasson M, Bibb M.
643   2003. Cloning and engineering of the cinnamycin biosynthetic gene cluster from
644   *Streptomyces cinnamoneus cinnamoneus* DSM 40005. Proc Natl Acad Sci U
645   S A 100:4316-4321.

646   25.   Iwamoto K, Hayakawa T, Murate M, Makino A, Ito K, Fujisawa T, Kobayashi T.
647   2007. Curvature-dependent recognition of ethanolamine phospholipids by
648   duramycin and cinnamycin. Biophys J 93:1608-1619.

21

26. Arnison PG, Bibb MJ, Bierbaum G, Bowers AA, Bugni TS, Bulaj G, Camarero JA, Campopiano DJ, Challis GL, Clardy J, Cotter PD, Craik DJ, Dawson M, Dittmann E, Donadio S, Dorrestein PC, Entian KD, Fischbach MA, Garavelli JS, Goransson U, Gruber CW, Haft DH, Hemscheidt TK, Hertweck C, Hill C, Horswill AR, Jaspars M, Kelly WL, Klinman JP, Kuipers OP, Link AJ, Liu W, Marahiel MA, Mitchell DA, Moll GN, Moore BS, Muller R, Nair SK, Nes IF, Norris GE, Olivera BM, Onaka H, Patchett ML, Piel J, Reaney MJ, Rebuffat S, Ross RP, Sahl HG, Schmidt EW, Selsted ME, et al. 2013. Ribosomally synthesized and post-translationally modified peptide natural products: overview and recommendations for a universal nomenclature. Nat Prod Rep 30:108-60.

27. Chatterjee C, Paul M, Xie L, van der Donk WA. 2005. Biosynthesis and Mode of Action of Lantibiotics. Chem Rev 105:633-684.

28. Kodani S, Komaki H, Ishimura S, Hemmi H, Ohnishi-Kameyama M. 2016. Isolation and structure determination of a new lantibiotic cinnamycin B from *Actinomadura atramentaria* based on genome mining. J Ind Microbiol Biotechnol 43:1159-65.

29. Shotwell OL, Stodola FH, Michael WR, Lindenfelser LA, Dworschack RG, Pridham TG. 1958. Antibiotics against plant disease. III. Duramycin, a new antibiotic from *Streptomyces cinnamomeus* forma *azacoluta*. J Am Chem Soc 80:3912-3915.

30. Marki F, Hanni E, Fredenhagen A, van Oostrum J. 1991. Mode of action of the lanthionine-containing peptide antibiotics duramycin, duramycin B and C, and cinnamycin as indirect inhibitors of phospholipase A2. Biochem Pharmacol 42:2027-35.

31. Chen E, Chen Q, Chen S, Xu B, Ju J, Wang H. 2017. Mathermycin, a Lantibiotic from the Marine Actinomycete *Marinactinospora thermotolerans* Appl Environ Microbiol 83.

32. Ökesli A, Cooper LE, Fogle EJ, van der Donk WA. 2011. Nine Post-translational Modifications during the Biosynthesis of Cinnamycin. J Am Chem Soc 133:13753-13760.

33. Huo L, Okesli A, Zhao M, van der Donk WA. 2017. Insights into the Biosynthesis of Duramycin. Appl Environ Microbiol 83.

34. Xie L, van der Donk WA. 2004. Post-translational modifications during lantibiotic biosynthesis. Curr Opin Chem Biol 8:498-507.

683   35.   Oliynyk I, Varelogianni G, Roomans GM, Johannesson M. 2010. Effect of
684   duramycin on chloride transport and intracellular calcium concentration in cystic
685   fibrosis and non-cystic fibrosis epithelia. Apmis 118:982-990.

686   36.   Holmes NA, Devine R, Qin Z, Seipke RF, Wilkinson B, Hutchings MI. 2018.
687   Complete genome sequence of *Streptomyces formicae KY5*, the formicamycin
688   producer. J Biotechnol 265:116-118.

689   37.   Blin K, Wolf T, Chevrette MG, Lu X, Schwalen CJ, Kautsar SA, Suarez Duran
690   HG, De Los Santos EL, Kim HU, Nave M. 2017. antiSMASH 4.0—
691   improvements in chemistry prediction and gene cluster boundary identification.
692   Nucleic Acids Res 45:W36-W41.

693   38.   O'Rourke S, Widdick D, Bibb M. 2017. A novel mechanism of immunity controls
694   the onset of cinnamycin biosynthesis in *Streptomyces cinnamoneus* DSM
695   40646. J Ind Microbiol Biotechnol 44:563-572.

696   39.   Andexer JN, Kendrew SG, Nur-e-Alam M, Lazos O, Foster TA, Zimmermann
697   A-S, Warneck TD, Suthar D, Coates NJ, Koehn FE, Skotnicki JS, Carter GT,
698   Gregory MA, Martin CJ, Moss SJ, Leadlay PF, Wilkinson B. 2011. Biosynthesis
699   of the immunosuppressants FK506, FK520, and rapamycin involves a
700   previously undescribed family of enzymes acting on chorismate. Proc Natl Acad
701   Sci U S A 108:4776-4781.

702   40.   Gomez-Escribano JP, Bibb MJ. 2011. Engineering *Streptomyces coelicolor* for
703   heterologous expression of secondary metabolite gene clusters. Microbial
704   Biotechnology 4:207-215.

705   41.   Hong H-J, Hutchings MI, Hill LM, Buttner MJ. 2005. The role of the novel Fem
706   protein VanK in vancomycin resistance in *Streptomyces coelicolor*. J Biol Chem
707   280:13055-13061.

708   42.   Bierman M, Logan R, O'Brien K, Seno E, Rao RN, Schoner B. 1992. Plasmid
709   cloning vectors for the conjugal transfer of DNA from *Escherichia coli* to
710   *Streptomyces* spp. Gene 116:43-49.

711   43.   Lopatniuk M, Myronovskyi M, Luzhetskyy A. 2017. *Streptomyces albus*: A New
712   Cell Factory for Non-Canonical Amino Acids Incorporation into Ribosomally
713   Synthesized Natural Products. ACS Chem Biol 12:2362-2370.

714   44.   Kieser T, Foundation JI, Bibb MJ, Buttner MJ, Chater KF, Hopwood DA. 2000.
715   Practical *Streptomyces* Genetics. John Innes Foundation.
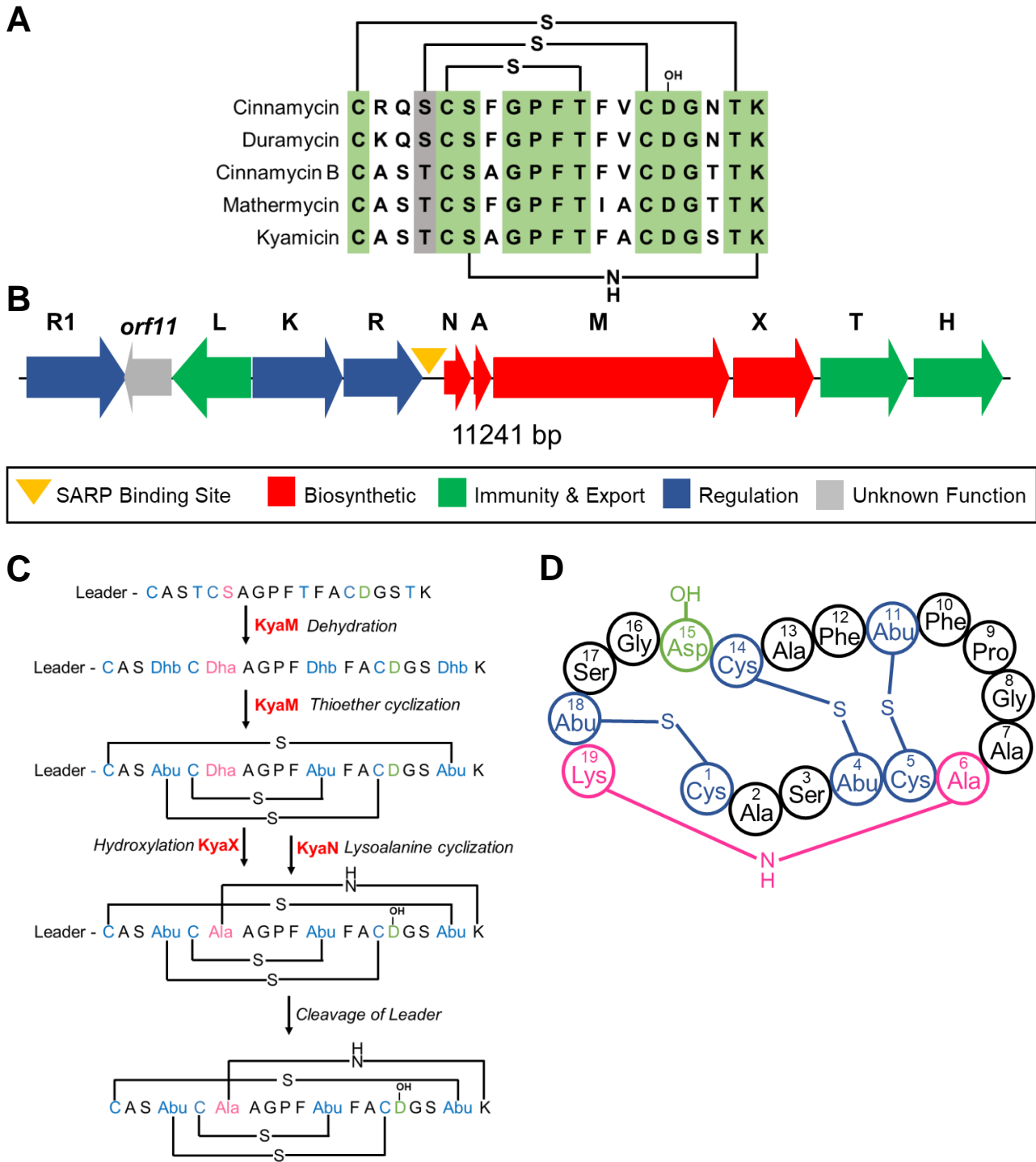
FIG 1 Kyamicin peptide sequence and biosynthesis. (A) Alignment of core peptides of kyamicin and a selection of known Type B cinnamycin-like lantibiotics, with the positions of the thioether and lysinoalanine bridges in the mature peptide shown. Conserved residues are highlighted in green, similar residues are highlighted in grey. **(B)** The kyamicin biosynthetic gene cluster, with genes colored according to predicted function. **(C)** Schematic of kyamicin biosynthesis. The thioether bridges are formed first by dehydration of Thr4, Thr11, Thr18 and Ser6 by KyaM to form dehydrobutyrine (Dhb) and dehydroalanine (Dha) residues, respectively. After thioether cyclization by KyaM, Dhb becomes S-linked Abu and Dha becomes S-linked Ala. Asp15 is hydroxylated by KyaX and the lysinoalanine bridge is then formed between Dha6 and Lys19 by KyaN. After the core peptide is fully modified, the leader peptide is proteolytically cleaved. **(D)** Structural representation of the mature kyamicin lantibiotic.
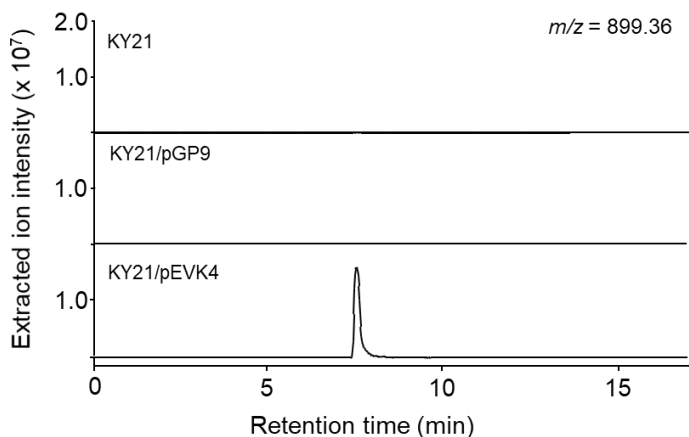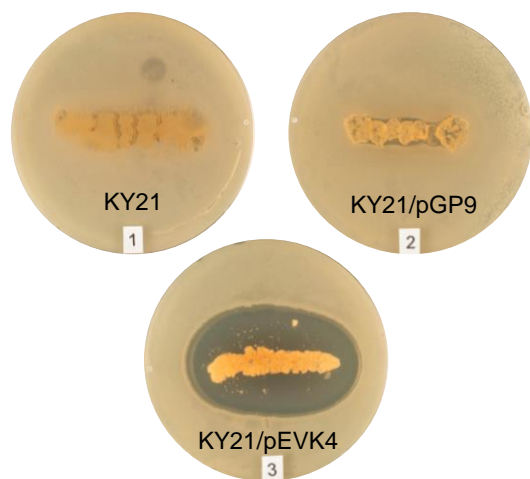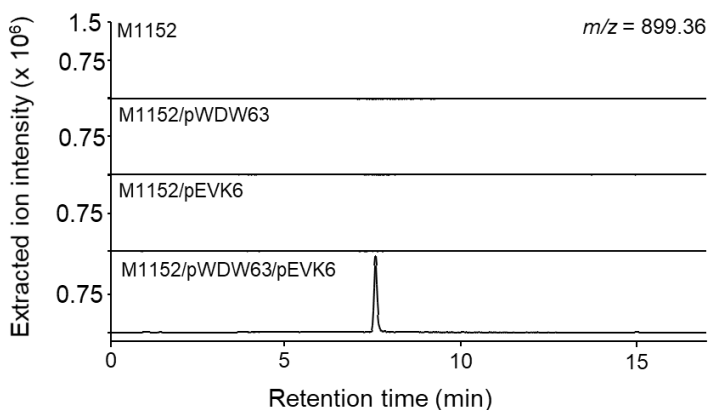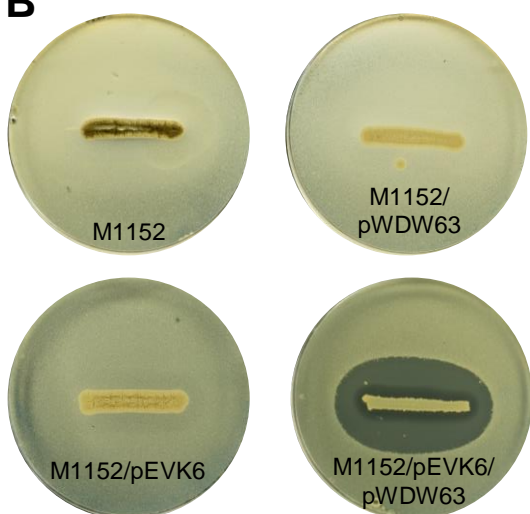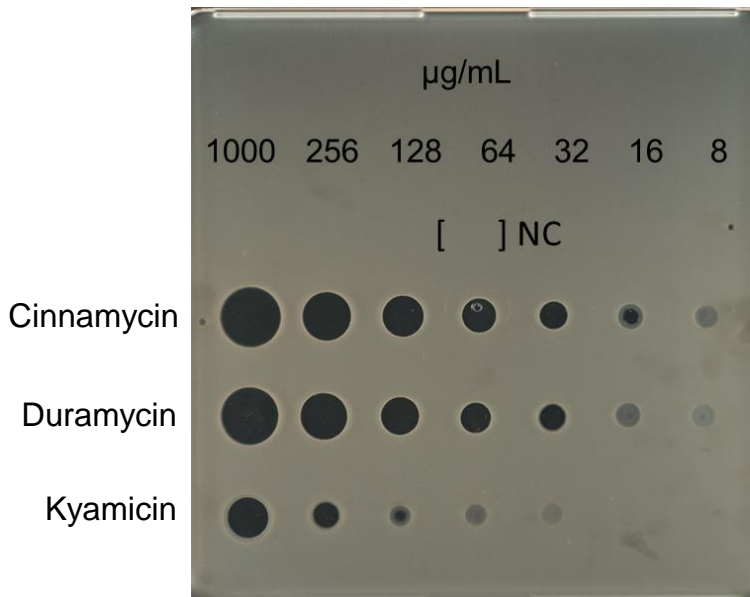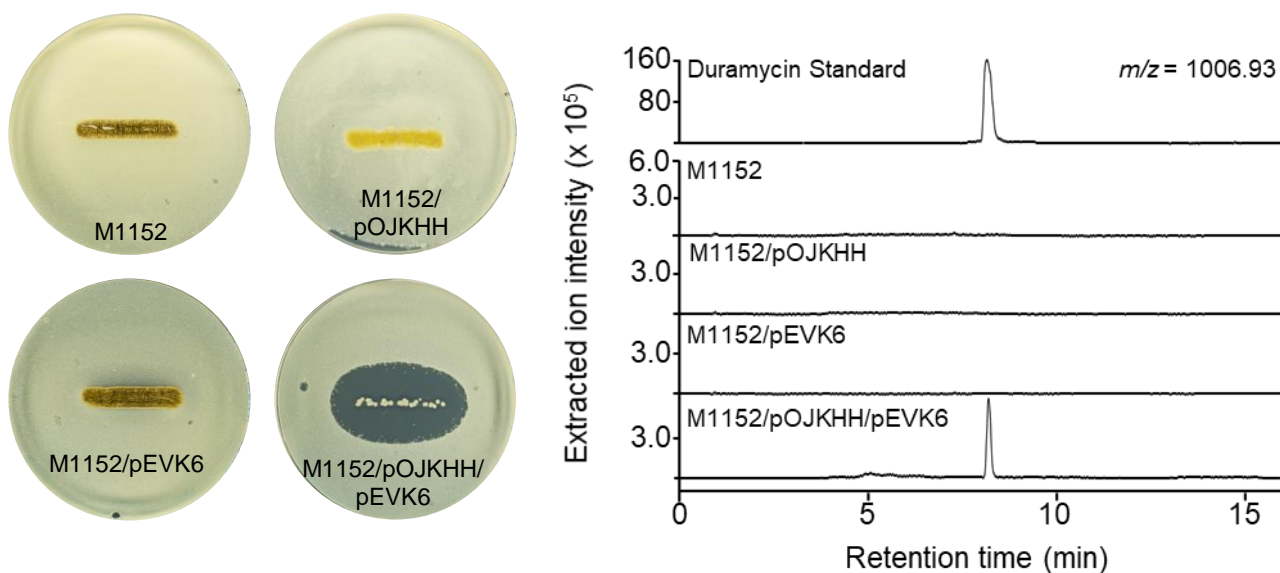
FIG 2 Activation of kyamicin biosynthesis and heterologous expression. Overlay bioassays were carried out with *B. subtilis* EC1524 and agar plugs were taken adjacent to the central streak and analysed by UPLC/MS. Extracted ion chromatograms are shown where m/z = 899.36 ([M + 2H]$^{2+}$). Images and LC traces are representative of at least three biological repeats. **(A)** Activation of kyamicin production in KY21 strains. The pEVK4 vector containing *kyaR1* and *kyaL* results in a zone of inhibition, corresponding to the production of kyamicin, in contrast to the pGP9 empty vector control or the wildtype strain. **(B)** Heterologous expression of kyamicin in *S. coelicolor* M1152. A zone of inhibition, corresponding to kyamicin production, is observed only when the pWDW63 carrying the *kya* biosynthetic genes is expressed in combination with pEVK6 carrying *kyaR1* and *kyaL.*
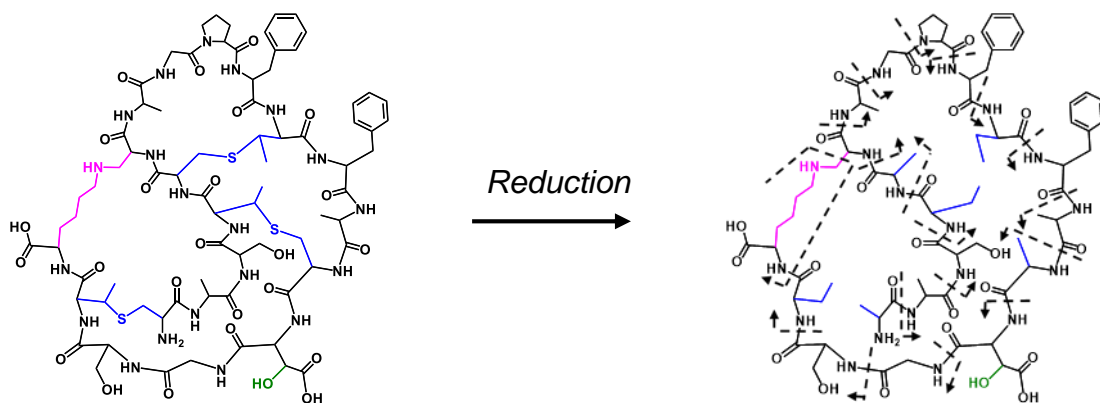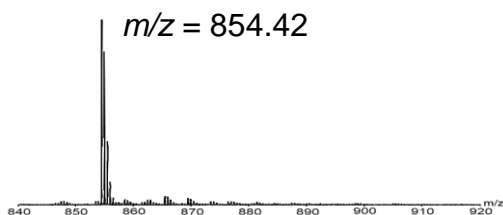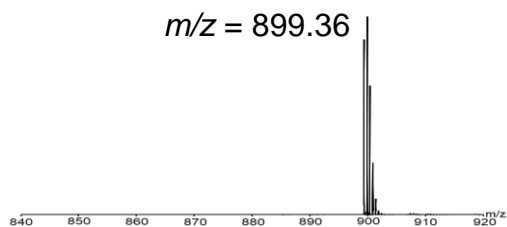
FIG 3 Characterisation of kyamicin. The connectivity of the peptide was confirmed by chemical reduction followed by tandem MS fragmentation. Reduction with $NaBH_4$-$NiCl_2$ resulted in the cleavage of the methyllanthionine bridges (blue), corresponding to the loss of three S atoms and gain of six H atoms, with a mass shift from $[M + 2H]^{2+}$ = 899.36 m/z to 854.42 m/z. Tandem MS using the MALDI-ToF LIFT method allowed identification of the y ion (NH_3^+) series for the complete peptide (Figure S5). Fragmentation of the lysinoalanine bridge (pink) occurred via rearrangement to give $N=CH_2$ at the terminus of the lysine sidechain and a glycine residue at position 6.

FIG 4 Comparative bioassay of kyamicin, duramycin and cinnamycin against _B. subtilis_ EC1524. The MIC of each substance was determined by direct application of serial dilutions of the compounds in water on a SNA plate inoculated with _B. subtilis_ EC1524. NC = H_2O as the negative control. The MIC of kyamicin is 128 μg/mL, whereas duramycin inhibits at 32 μg/mL and cinnamycin at 16 μg/mL.

FIG 5 Activation of duramycin biosynthesis. Overlay bioassays were carried out with *B. subtilis* EC1524 and agar plugs were taken adjacent to the central streak and analysed by UPLC/MS. Extracted ion chromatograms are shown where *m/z* = 1006.93 ([M + 2H]$^{2+}$). Duramycin was only detected in the strain carrying both pOJKHH and pEVK6. The duramycin peak aligns with an authentic standard of duramycin (1 mg/mL in 5% formic acid), shown on a separate scale. Images and LC traces are representative of at least three biological repeats.

TABLE 1. Proteins encoded by the kyamicin, cinnamycin and duramycin BGCs.

Kyamicin	Cinnamycin	Duramycin	Proposed function
KyaN (123aa)	CinN (119aa)	DurN (119aa)	Formation of lysinoalanine bridge
KyaA (78aa)	CinA (78aa)	DurA (77aa)	Precursor peptide
KyaM (1065aa)	CinM (1088aa)	DurM (1083aa)	Formation of lanthionine residues
KyaX (302aa)	CinX (325aa)	DurX (327aa)	Hydroxylation of Asp15
KyaT (327aa)	CinT (309aa)	DurT (352aa)	Export
KyaH (294aa)	CinH (290aa)	DurH (290aa)	Export
Not Present	CinY	DurY	Not essential
Not present	CinZ	DurZ	Not essential
Not present	Cinorf8	Durorf8	Not essential
Not present	Cinorf9	Not present	Not essential
KyaR (216aa)	CinR (216aa)	DurR (216aa)	Regulation
KyaK (372aa)	CinK (354aa)	DurK (349aa)	Regulation
KyaL (226aa)	CinL (236aa)	DurL (235aa)	Immunity
Kyaorf11 (295aa)	Cinorf11 (396aa)	Durorf11 (396aa)	Not essential
KyaR1 (260aa)	CinR1 (261aa)	DurR1 (261aa)	Regulation

TABLE 2. Calculated and observed *m/z* values for lantibiotic compounds in this study

Compound	Formula	Calculated [M + 2H]$^{2+}$ *m/z*	Observed [M + 2H]$^{2+}$ *m/z*	Error (ppm)
Kyamicin	$C_{76}H_{108}N_{20}O_{25}S_3$	899.3551	899.3553	0.22
Deoxykyamicin	$C_{76}H_{108}N_{20}O_{24}S_3$	891.3576	891.3557	-2.13
Partially Reduced Kyamicin	$C_{76}H_{110}N_{20}O_{25}S_2$	884.3768	884.3767	-0.11
Partially Reduced Kyamicin	$C_{76}H_{112}N_{20}O_{25}S$	869.3987	869.3990	0.35
Reduced Kyamicin	$C_{76}H_{114}N_{20}O_{25}$	854.4204	854.4202	-0.23
Duramycin	$C_{89}H_{125}N_{23}O_{25}S_3$	1006.9262	1006.9232	-2.98
Deoxyduramycin	$C_{89}H_{125}N_{23}O_{24}S_3$	998.9287	998.9253	-3.40